1. Mixing Ratio and Uncertainty Calculation

Mixing ratios were calculated, in the absence of suitable reference materials, according to Equation S1.

$$R_{ppb} = \frac{RH^{+} \times 10^{9} \times U \times 2.8 \times 22400 \times 1013^{2} \times T^{2} \times Tr_{(H_3{}^{18}O^{+})}}{k \times 9.2^{2} \times H_3{}^{18}O^{+} \times 500 \times P^{2} \times 6.02 \times 10^{23} \times 273.15^{2} \times Tr_{(RH^{+})}} \quad \text{(S1)}$$

Where R_{ppb} is the mixing ratio of the analyte ion R, RH^{+} is the raw signal of the protonated analyte in cps, 10^9 is the conversion to ppb, U is the voltage of the drift tube in volts, 2.8 is the reduced ion mobility (which has been experimentally determined) in cm^2/Vs, 22400 is the molar volume in moles per cm^3, 1013 is standard pressure in mbar, T is the temperature of the drift tube in K, $Tr_{(H318O+)}$ is the transmission of the primary ion isotope ($H_3{}^{18}O^{+}$), k is the rate reaction coefficient of the analyte ion with the hydronium ion, 9.2 is the length of the drift tube in cm, $H_3{}^{18}O^{+}$ is the raw signal of the isotope of the primary ion, 500 is the isotopic ratio correction factor, P is the pressure of the drift tube in mbar, 6.02×10^{23} is Avogadro's number in molecules per mole, 273.15 is standard temperature, and $Tr_{(RH+)}$ is the transmission of the protonated analyte ion. The isotope of the primary ion is used to avoid detector saturation. It must be noted that due to the backreaction of formaldehyde with water vapor in the drift tube, mixing ratios of formaldehyde are likely a lower limit (Holzinger et al., 2019; Hansel et al., 1997). However, due to the low absolute humidity levels in the Arctic, this reaction is negligible, furthermore, no correlation was observed between humidity (absolute or relative) and formaldehyde.

In the absence of suitable reference materials, an uncertainty budget was created based on the formula for kinetic calibration Eq. (S1). There are terms in Eq. (S1) that are assumed negligible including drift temperature, drift pressure, and ion transmission. These components are deemed negligible because they either are measured with high accuracy (temperature and pressure) or are lacking empirical error analysis (ion transmission). The greatest sources of uncertainty in this equation are the rate reaction coefficient and the counts of the primary ion and the analyte ion. According to Cappellin et al. (2010), the relative uncertainty of their rate reaction coefficients is stated at 15 %. The uncertainty from the raw ion cps was determined from the counting statistics by assuming a Poisson distribution (Hayward et al., 2002). The standard uncertainty for the ion counts is, therefore, the square root of the cps multiplied by the signal integration time (5 sec). The analyte signal was blank corrected before uncertainty analysis. The expanded uncertainty is then calculated according to Eq. (S2), using a coverage factor of two.

$$U = 2 \times VMR \times \sqrt{0.15^{2} + \left(\frac{\sqrt{I_P}}{I_P}\right)^{2} + \left(\frac{\sqrt{I_{S-b}}}{I_{S-b}}\right)^{2}} \quad \text{(S2)}$$

Where U is the expanded uncertainty, VMR is the volume-mixing ratio, I_p is the raw counts of the primary ion, $I_{S\text{-}b}$ is the blank corrected counts of the analyte ion.

Table S1. Statistics for meteorological parameters (mean ± s.d.) for all seasons, spring (April 1 – June 8), summer (June 9 – August 6), and autumn (August 7 – October 31).

	All Seasons	Spring	Summer	Fall
Wind Direction / °	207.5 ± 89.0	202.4 ± 91.8	189.3 ± 2.6	223.8 ± 81.2
Wind Speed / m s^{-1}	3.3 ± 2.6	3.1 ± 2.4	3.5 ± 2.4	3.4 ± 2.7
Temperature / °C	-6.5 ± 9.6	-13.8 ± 9.0	2.2 ± 4.1	-7.0 ± 7.9
RH / %	77.4 ± 12.6	74.6 ± 10.6	78.0 ± 15.6	79.1 ± 11.4
Radiation / W m^{-2}	174.9 ± 163.9	222.3 ± 146.3	295.9 ± 4.2	57.0 ± 97.4
Pressure / hPa	1010.6 ± 9.0	1014.8 ± 8.6	1007.5 ± 6.5	1009.6 ± 9.5
Snow Depth / m	0.9 ± 0.6	1.4 ± 0.1	1.1 ± 0.4	0.3 ± 0.4

Table S2: Pearson correlation coefficients for chemical species, temperature and sun radiation measured during April at VRS. All correlations, apart from the numbers typed in italics, have linear regression p-values below 0.01.

April 2018	Formal-dehyde	Aceto-nitrile	Formic Acid	Acetone	Acetic Acid	Dimethyl Sulfide	Methyl Ethyl Ketone	Benzene	Propionic Acid	Tempe-rature	Radiation	Ozone
Formaldehyde	1.00											
Acetonitrile	0.70	1.00										
Formic Acid	0.76	0.45	1.00									
Acetone	0.40	0.30	*-0.03*	1.00								
Acetic Acid	-0.63	-0.74	-0.45	-0.32	1.00							
Dimethyl Sulfide	-0.47	-0.67	-0.16	-0.55	0.84	1.00						
Methyl Ethyl Ketone	0.52	0.20	0.76	0.03	-0.27	-0.07	1.00					
Benzene	0.27	0.04	0.70	-0.43	*-0.07*	0.24	0.84	1.00				
Propionic Acid / Methyl Acetate	-0.52	-0.66	-0.25	-0.41	0.90	0.94	-0.15	0.11	1.00			
Temperature	-0.47	-0.34	-0.75	0.16	0.54	0.23	-0.74	-0.77	0.46	1.00		
Radiation	-0.26	-0.26	-0.38	0.28	0.20	*0.06*	-0.25	-0.34	0.21	0.34	1.00	
Ozone	-0.52	-0.48	-0.21	-0.83	0.56	0.64	-0.26	0.15	0.59	0.17	-0.12	1.00

Table S3: Pearson correlation coefficients for chemical species, temperature and sun radiation measured during July at VRS. All correlations, apart from the numbers typed in italics, have linear regression p-values below 0.01.

July 2018	Formal-dehyde	Aceto-nitrile	Formic Acid	Acetone	Acetic Acid	Dimethyl Sulfide	Methyl Ethyl Ketone	Benzene	Propionic Acid / Methyl Acetate	Tempe-rature	Radiation	Ozone
Formaldehyde	1.00											
Acetonitrile	0.71	1.00										
Formic Acid	0.88	0.57	1.00									
Acetone	0.86	0.89	0.82	1.00								
Acetic Acid	0.85	0.58	0.95	0.85	1.00							
Dimethyl Sulfide	0.36	*0.01*	0.50	0.23	0.42	1.00						
Methyl Ethyl Ketone	0.85	0.55	0.93	0.81	0.97	0.41	1.00					
Benzene	0.57	0.50	0.50	0.61	0.59	0.26	0.60	1.00				
Propionic Acid / Methyl Acetate	0.83	0.57	0.95	0.82	0.97	0.39	0.95	0.50	1.00			
Temperature	0.65	0.85	0.54	0.82	0.58	*0.08*	0.54	0.45	0.54	1.00		
Radiation	0.49	0.23	0.59	*0.40*	0.51	0.26	0.53	0.15	0.56	0.31	1.00	
Ozone	0.54	0.82	0.39	*0.69*	0.39	0.18	0.33	0.43	0.33	0.76	0.07	1.00

Table S4: Pearson correlation coefficients for chemical species, temperature and sun radiation measured during September at VRS. All correlations, apart from the numbers typed in italics, have linear regression p-values below 0.01.

September 2018	Formal-dehyde	Aceto-nitrile	Formi c Acid	Acetone	Acetic Acid	Dimethyl Sulfide	Methyl Ethyl Ketone	Benzene	Propionic Acid/Methyl Acetate	Tempe -rature	Radiation	Ozone
Formaldehyde	1.00											
Acetonitrile	0.61	1.00										
Formic Acid	0.76	0.45	1.00									
Acetone	0.72	0.96	0.57	1.00								
Acetic Acid	*0.06*	0.29	*0.07*	0.28	1.00							
Dimethyl Sulfide	-0.29	-0.76	-0.18	-0.68	-0.10	1.00						
Methyl Ethyl Ketone	0.82	0.71	0.64	0.79	0.43	-0.35	1.00					
Benzene	0.50	0.15	0.42	0.19	0.21	0.25	0.61	1.00				
Propionic Acid / Methyl Acetate	0.76	0.35	0.62	0.43	0.12	*-0.03*	0.69	0.64	1.00			
Temperature	-0.81	-0.35	-0.77	-0.53	0.26	0.10	-0.58	-0.40	-0.68	1.00		
Radiation	*-0.07*	*-0.04*	-0.09	-0.06	0.29	-0.07	*0.01*	-0.11	-0.10	0.33	1.00	
Ozone	0.74	0.70	0.63	0.79	0.14	-0.26	0.72	0.31	0.56	-0.64	-0.23	1.00

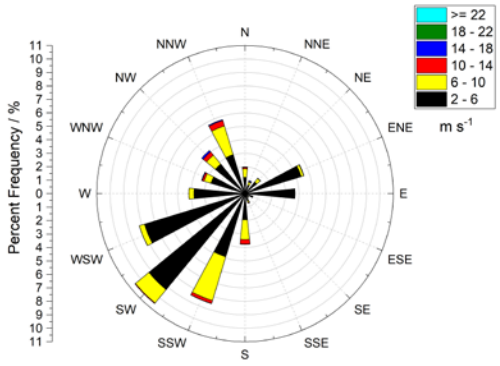

Fig. S1. Wind Rose for mean wind speed at 30 min time resolution over the sampling period. The y-axis represents the percent frequency of wind direction in percent and the colors indicate mean wind speed in m s^{-1}.

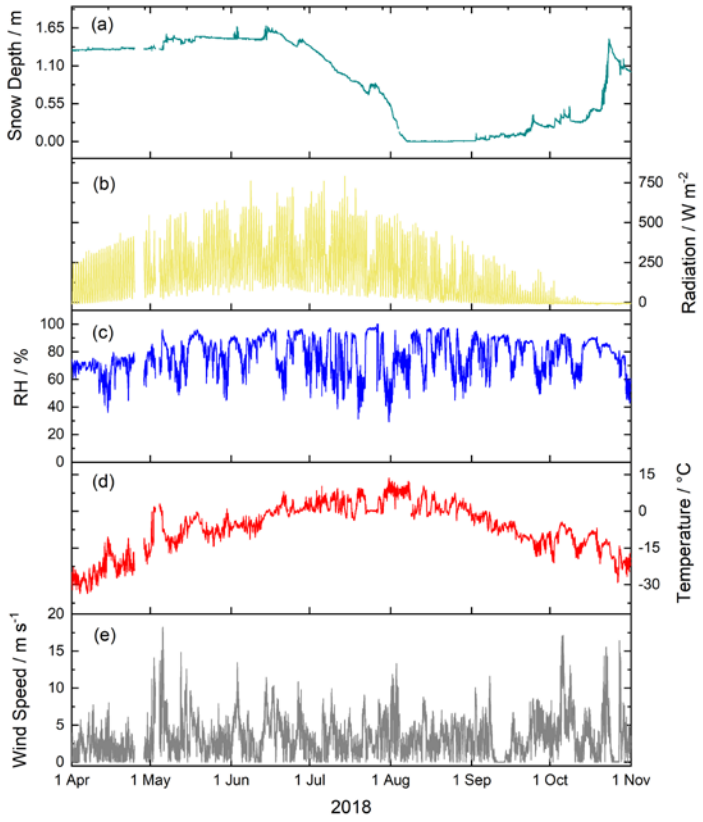

Fig. S2. Time series meteorological parameters **(a)** snow depth, **(b)** radiation, **(c)** relative humidity (RH), **(d)** temperature, and **(e)** wind speed during the entire measurement period.

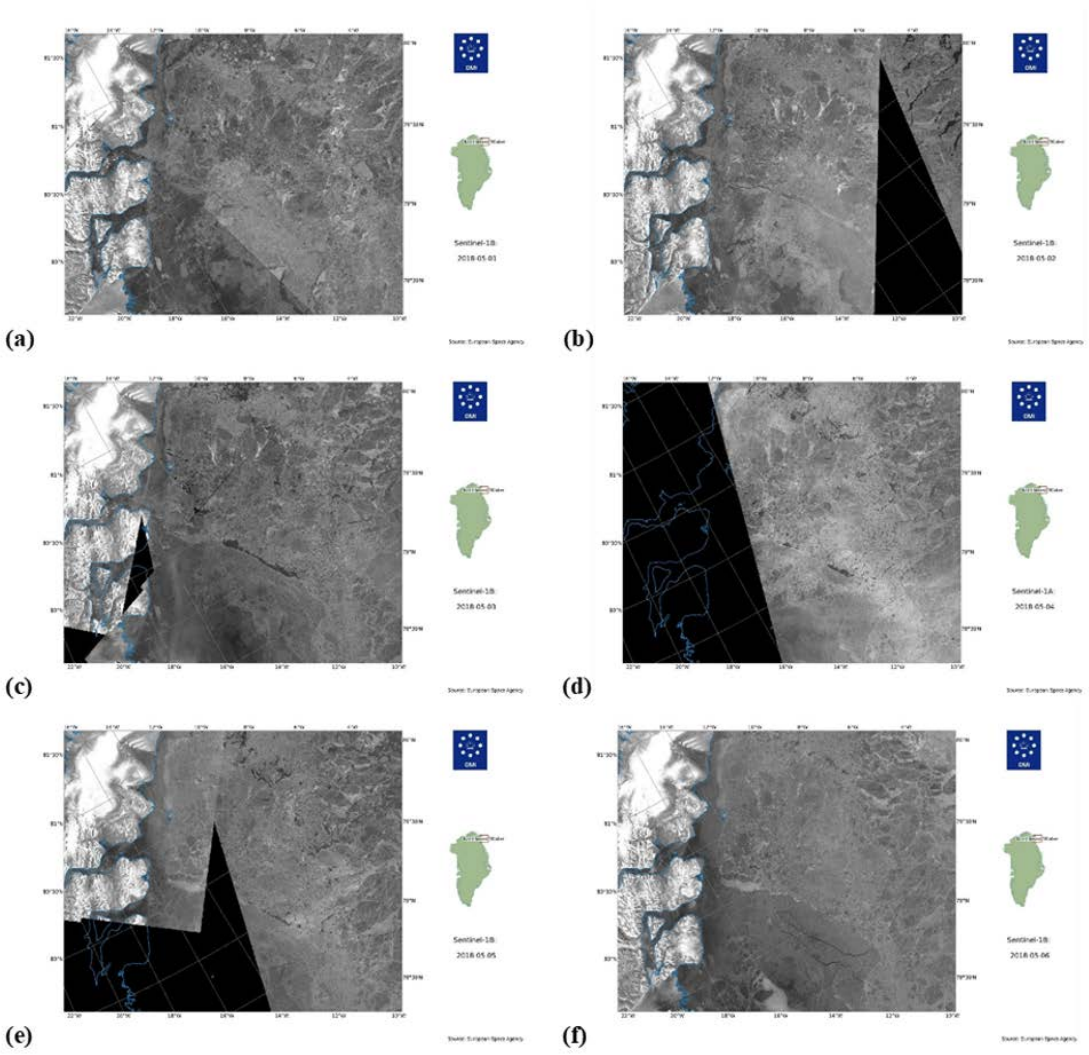

Fig. S4. Satellite images from Sentinel 1-B, delivered by the University of Dundee, Scotland and NASA's Goddard Space Flight Center; **(a)** May 1st **(b)** May 2nd **(c)** May 3rd **(d)** May 4th **(e)** May 5th **(f)** May 6th. The presence of open leads can be seen southwest of VRS at approx. 79° 30´ N and 12° W.

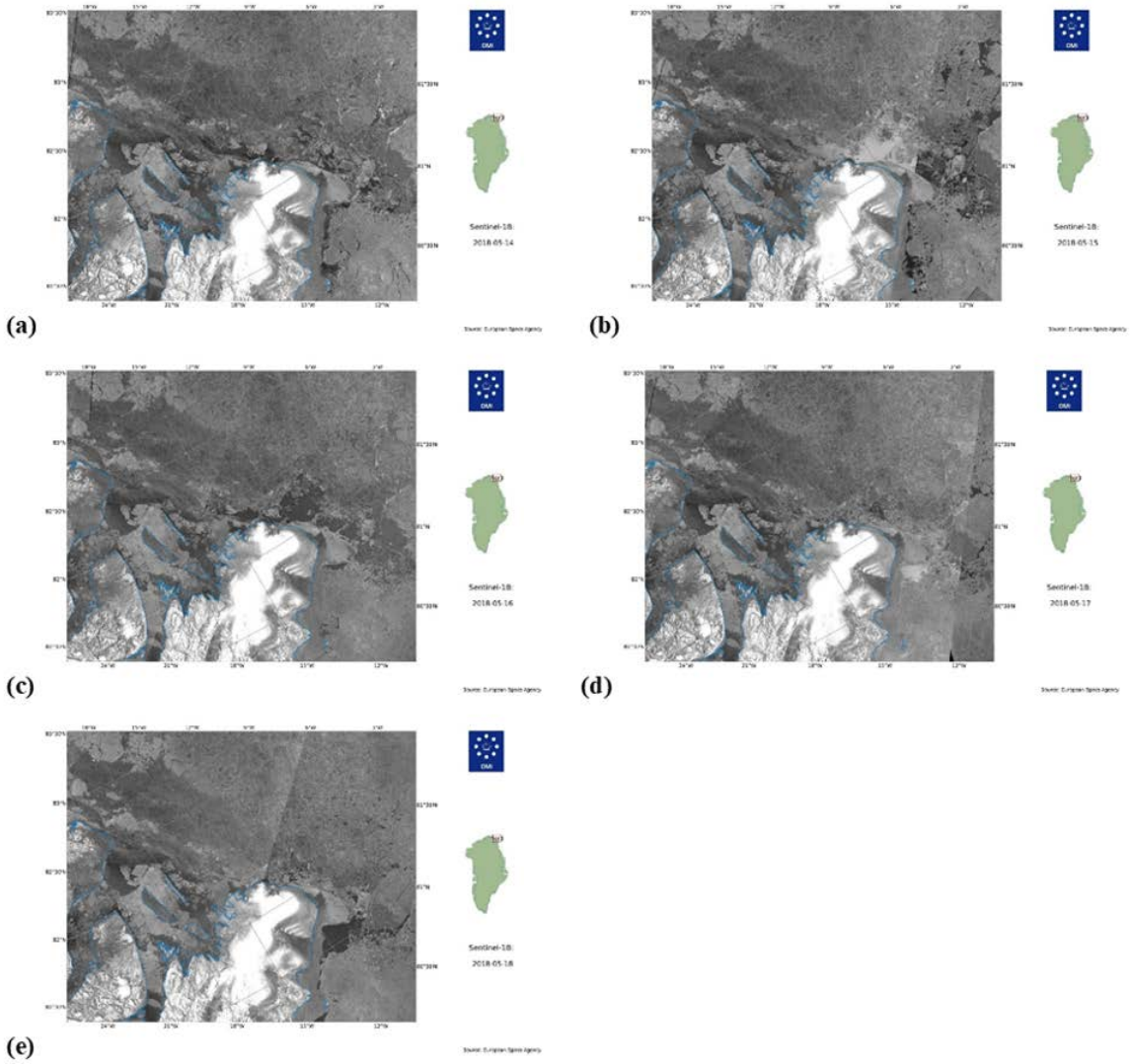

Fig. S5. Satellite images from Sentinel 1-B, delivered by the University of Dundee, Scotland and NASA's Goddard Space Flight Center; **(a)** May 14th **(b)** May 15th **(c)** May 16th **(d)** May 17th **(e)** May 18th. The presence of open leads can be seen northeast of VRS at approx. 81° 50´ N and 10° W as well as southwest of VRS at approx. 81° N and 12° W.

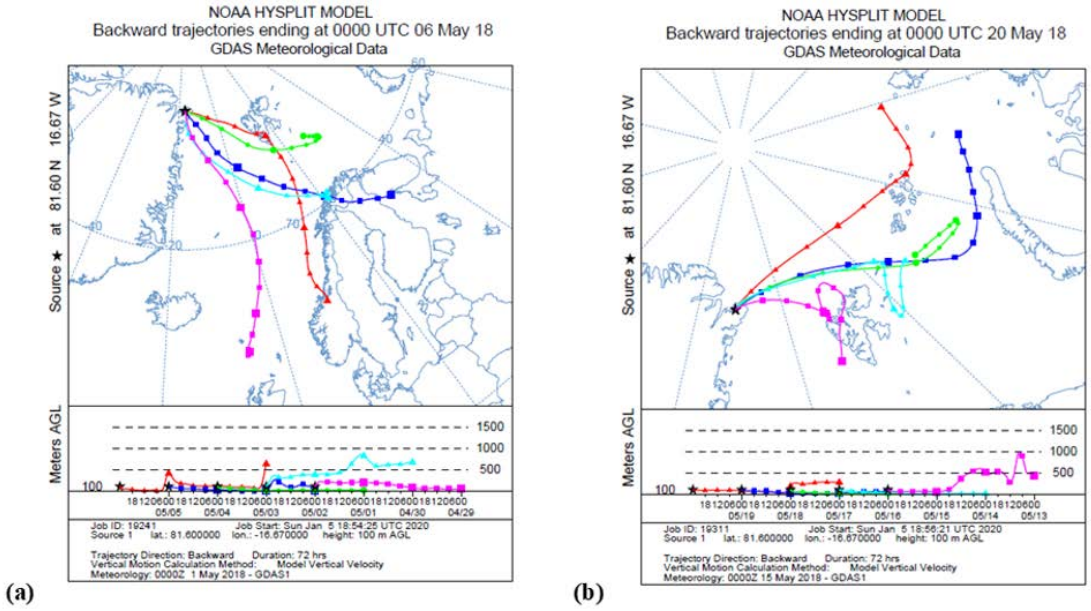

80

Fig. S6. HYSPLIT back trajectory analysis for **(a)** May 1st – 6th **(b)** May 16th-20th arriving at 100 m above ground level extending 72 hours backward in time. A new trajectory was every 24 hours.

85

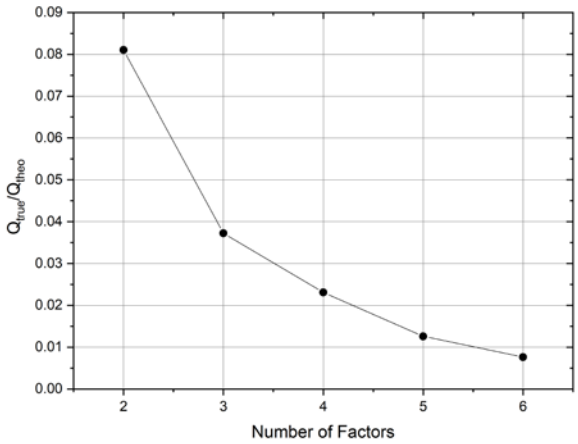

Fig. S7. The ratio of Q_{true} to Q_{theo} versus the number of factors.

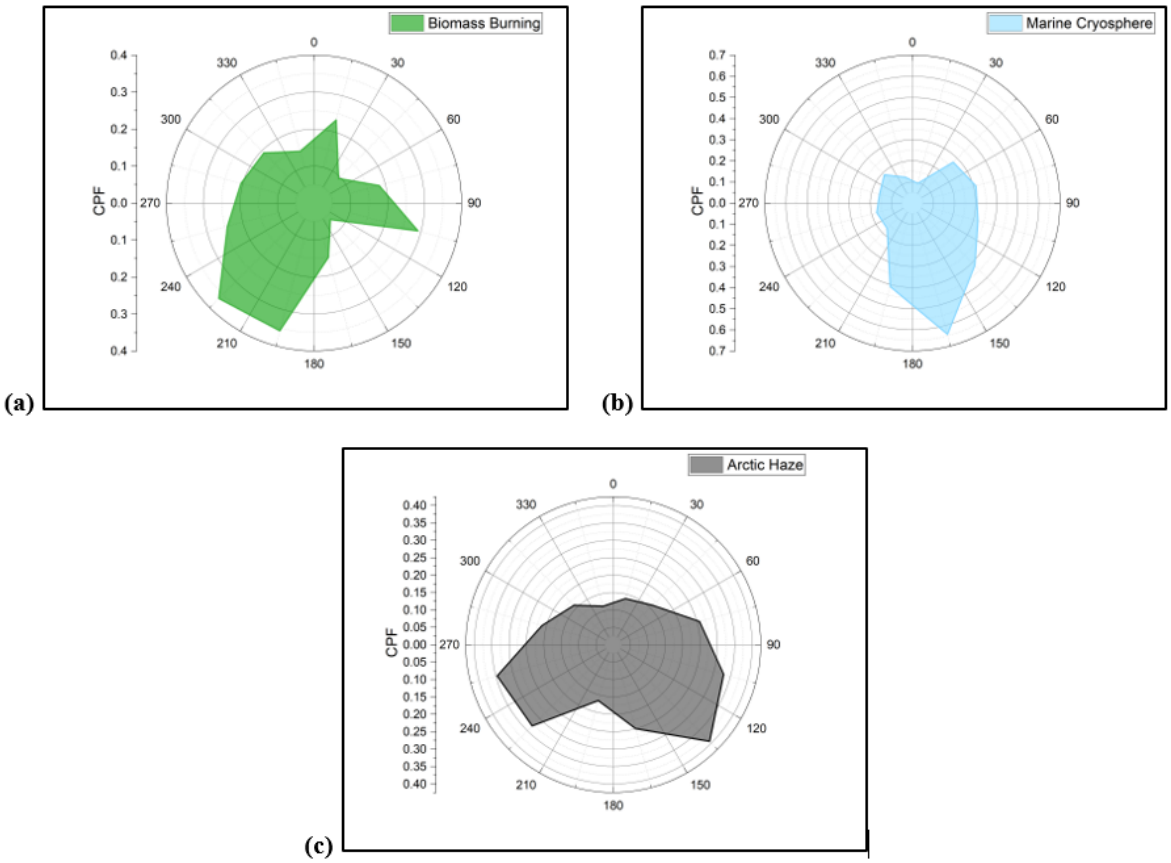

Fig. S8. Conditional probability function roses for **(a)** Biomass Burning Factor, **(b)** Marine Cryosphere Factor, and **(c)** Arctic Haze Factor.

References

Cappellin, L., Probst, M., Limtrakul, J., Biasioli, F., Schuhfried, E., Soukoulis, C., Märk, T. D., and Gasperi, F.: Proton transfer reaction rate coefficients between H3O+ and some sulphur compounds, International Journal of Mass Spectrometry, 295, 43-48, 10.1016/j.ijms.2010.06.023, 2010.

Hansel, A., Singer, W., Wisthaler, A., Schwarzmann, M., and Lindinger, W.: Energy dependencies of the proton transfer reactions H3O+ + CH2O ⇔ CH2OH+ + H2O, International Journal of Mass Spectrometry and Ion Processes, 167-168, 697-703, https://doi.org/10.1016/S0168-1176(97)00128-6, 1997.

Hayward, S., Hewitt, C. N., Sartin, J. H., and Owen, S. M.: Performance characteristics and applications of a proton transfer reaction-mass spectrometer for measuring volatile organic compounds in ambient air, Environmental Science & Technology, 36, 1554-1560, 10.1021/es0102181, 2002.

Holzinger, R., Acton, W. J. F., Bloss, W. J., Breitenlechner, M., Crilley, L. R., Dusanter, S., Gonin, M., Gros, V., Keutsch, F. N., Kiendler-Scharr, A., Kramer, L. J., Krechmer, J. E., Languille, B., Locoge, N., Lopez-Hilfiker, F., Materić, D., Moreno, S., Nemitz, E., Quéléver, L. L. J., Sarda Esteve, R., Sauvage, S., Schallhart, S., Sommariva, R., Tillmann, R., Wedel, S., Worton, D. R., Xu, K., and Zaytsev, A.: Validity and limitations of simple reaction kinetics to calculate concentrations of organic compounds from ion counts in PTR-MS, Atmospheric Measurement Techniques, 12, 6193-6208, 10.5194/amt-12-6193-2019, 2019.